J. Fluid Mech. (1992), *vol.* 239, *pp.* 489–509
Printed in Great Britain

Transition to a periodic regime in mixed convection in a square cavity

By ELIAS PAPANICOLAOU AND YOGESH JALURIA
Department of Mechanical & Aerospace Engineering, Rutgers, The State University of New Jersey, New Brunswick, NJ 08903, USA

(Received 5 November 1991)

The numerical study presented in this work describes the transition from a steady, laminar regime to a periodic regime in an air-filled, two-dimensional cavity subjected to localized heating. The cavity lies at the bottom of a horizontal channel through which a cold air stream flows. The heating is provided by a constant heat input source, located on one of the vertical walls of the cavity and this generates a buoyancy-driven recirculating flow in the cavity. The interaction of this recirculating flow with the cold through-flow leads to steady flow and thermal fields as long as the value of the Grashof number, associated with the heat input from the source, remains below a certain critical value. As this value is exceeded, an unstable situation arises and, after an initial transient, the results show a very regular, periodic, almost sinusoidal behaviour. Similar previous works on natural convective flows in cavities have discovered such a periodic behaviour, as a form of travelling wave instability, having the characteristics of a Hopf bifurcation. These characteristics were also found to be present in this mixed convective situation, where the amplitudes of the oscillating quantities, like the thermal energy outflow, vary with the square root of the Grashof number. However, the present problem is also governed by the value of the Reynolds number, and its effect on the results is studied. The observed instability is of thermal origin, with small fluid cells at the centre of the cavity being subjected to periodic cooling and heating and, therefore, to a circulatory motion due to the density change.

1. Introduction

It is well known today, from relatively recent findings, that natural convection in cavities, due to heating not only from below as in the Rayleigh–Bénard problem but also from the sides, exhibits oscillatory behaviour when the main governing parameter, the Rayleigh number, reaches a certain critical value. This value depends on the type of boundary conditions imposed at the horizontal walls of the cavity, i.e. whether adiabatic or perfectly conducting, as well as the aspect ratio, usually expressed as height over width of the cavity. The most notable works demonstrating this behaviour are those by Briggs & Jones (1985), Jones & Briggs (1986), LeQuéré & Alziary de Roquefort (1985, 1986) and Winters (1987). All these studies identified this transition as a Hopf bifurcation and as the first transition on the route to turbulence.

However, similar observations of periodic behaviour had already been made before the work mentioned above, in several experimental and numerical studies. Igarashi (1978) carried out an experimental investigation of the natural convection due to a line heat source placed along the centreline of a long horizontal enclosure. He

observed an oscillatory flow at a value of the modified Rayleigh number Ra^*, based on the strength or energy input of the heat source, in the range

$$6 \times 10^5 \leqslant Ra^* \leqslant 3 \times 10^8.$$

The frequency of the oscillations was found to vary as $Ra^{*0.40}$. Later, in a numerical study, Küblbeck, Merker & Straub (1980) found oscillatory results when they considered an enclosure with one sidewall heated to a high temperature up to half its height and to a lower temperature along the remaining half, with the other three walls kept adiabatic. Oscillations developed at a value of the Rayleigh number, based on the width L of the cavity, $Ra = 5.6 \times 10^5$ and their frequency was found to increase as $Ra^{0.5}$.

Meanwhile, the study of the transient behaviour of a fluid in a cavity heated from the sides by Patterson & Imberger (1980) helped later researchers to explain the physical mechanisms of the periodic behaviour which was observed in their work. They suggested that at high Rayleigh numbers, the presence of internal gravity waves is a determining factor in the time required for the attainment of steady-state conditions. These gravity waves are generated from the discharge of the upward-moving buoyancy-induced flow along the hot wall into the thermally stratified core of the cavity and are characterized by the Brunt–Väisälä frequency (Turner 1973). The steady state is achieved after the gravity waves are damped, at a time T_d of the order $T_d \approx h^2/\nu$, where h is the height of the cavity and ν the viscosity of the fluid. As was realized in later studies, the presence of internal waves in the cavity leads to the observed periodic behaviour.

The numerical work of Staehle & Hahne (1982), without any specific reference to the gravity waves, described the transient behaviour of fluids with different Prandtl numbers in both horizontal and vertical cavities. They observed an overshoot in the beginning, in both the values of the stream function at the centre of the cavity and the mean Nusselt number, and this was followed by oscillations that decayed in time and whose frequency was an increasing function of the Rayleigh number. For the cavity heated from the sides, the frequency varied with the square root of the Rayleigh number, in agreement with Küblbeck *et al.* (1980). The oscillations were characterized by a damping factor (the ratio between two successive maxima of the oscillating values), which decreases with Ra and eventually approaches the value of 1 at high values of Ra. At this point, the maximum amplitude remains constant with time and a steady periodic regime is attained.

Ivey (1984), in an experimental work where pure water and a mixture of glycerol and water were used as the working fluids, did not observe internal gravity waves, but instead, at high Rayleigh numbers, he observed an oscillatory behaviour which was more pronounced near the corners of the cavity. He attributed this phenomenon to an instability due to an internal hydraulic jump, as the boundary layer flows along the vertical walls impinged on the horizontal boundaries and turned towards the interior of the cavity as horizontal flows. These flows were characterized by a Froude number $Fr > 1$ and, therefore, they were supercritical and would undergo an internal hydraulic jump, as described by Turner (1973).

Air was the fluid used in the numerical work of LeQuéré & Alziary de Roquefort (1985). They considered aspect ratios between 4 and 10 and cavities with isothermal vertical walls and adiabatic horizontal walls. They determined the critical value of the Rayleigh number Ra_{cr} at which, for each aspect ratio, a transition from a steady to a time-dependent regime occurs. They found that at values $Ra \leqslant Ra_{cr}$, there were oscillations due to the internal gravity waves. These were eventually damped out and

a steady state was obtained, in agreement with the observations of Staehle & Hahne (1982). These oscillations may be characterized by two distinct frequencies. As Ra_{cr} is reached, the oscillations persist and the two frequencies are still present, until at a certain time the lower frequency disappears and the regime is characterized by a single frequency. The lower frequency was attributed to the presence of the internal gravity waves, and the higher frequency to the frequency of travelling waves. These were shown in contour line plots of the fluctuating temperature field. In a later work, LeQuéré & Alziary de Roquefort (1986) obtained numerical results for cavities with aspect ratios in the range 1–10, with isothermal vertical walls and either adiabatic or perfectly conducting horizontal walls. For both cases, they determined the critical values of the Rayleigh number for the transition to a periodic flow, as a function of the aspect ratio. The perfectly conducting walls had lower values of Ra_{cr} than the adiabatic walls at the same aspect ratio. For an aspect ratio of 1 and for perfectly conducting horizontal walls, they found a critical number of $Ra_{cr} = 2.2 \times 10^6$ in agreement with the results of Briggs & Jones (1985). They concluded that the transition to periodic convection had the characteristics of a Hopf bifurcation, where the frequency of the oscillations varies as $Ra^{0.5}$ and the amplitude of the limit cycle varies as $(Ra - Ra_{cr})^{0.5}$.

A square cavity with perfectly conducting top and bottom horizontal walls and heated from the sides was the configuration studied by Briggs & Jones (1985) and Jones & Briggs (1986). In the first study they presented experimental results and determined the onset of the periodic regime at $Ra = 3 \times 10^6$. As they further increased the Rayleigh number, a second, higher frequency appeared, then the low frequency disappeared and another, even higher frequency appeared which persisted until the value $Ra = 1.2 \times 10^7$, which was the last value reported. Briggs & Jones interpreted the periodic behaviour as a resonance between the travelling waves in the boundary layers along the vertical walls and the gravity waves due to the thermal stratification of the core of the cavity. In the second study (Jones & Briggs 1986), they presented both experimental and numerical results. Their numerical results showed a lower critical Rayleigh number but they confirmed the step changes in the frequency as Ra increased. The differences were attributed to three-dimensional effects in the experiment, since the numerical simulation was two-dimensional. The contour plots of the instantaneous temperature fields showed the existence of hot and cold cells following a circulatory motion inside the cavity. The transition to periodic flow was identified as a Hopf bifurcation.

Haldenwang (1986) also verified the presence of internal gravity waves during the transient state in his numerical simulation of convection in a cavity heated from the sides, with adiabatic horizontal walls. Damped oscillations were observed, with a single frequency for $Ra < 10^8$ and with two frequencies for $Ra = 10^8$. The frequencies were very close to the value of the Brunt–Väisälä frequency. For the aspect ratio of 1 considered, he did not find a steady periodic regime, but as the Rayleigh number reached the value of $10^{8.5}$, the flow became chaotic and no distinct frequency was present. The square cavity with perfectly conducting horizontal walls (Briggs & Jones 1985) was also studied by Winters (1987). In his linear stability analysis, he proved the existence of five Hopf bifurcation points in the range

$$2 \times 10^6 \leqslant Ra \leqslant 3 \times 10^6.$$

This was in agreement with the results of Briggs & Jones (1985) and Jones & Briggs (1986). Winters also claimed that the existence of these distinct points, corresponding to distinct frequencies of oscillation, may be associated with the excitation of

different modes of the internal gravity waves. This confirmed the argument of Briggs & Jones (1985) that the oscillations are due to a resonance between the travelling waves and the gravity waves. The bifurcation point corresponding to the lower value of Ra was found to be $Ra = 2.109 \times 10^6$ and this was taken as the value of Ra_{cr} for the transition to the periodic regime.

In a more recent work, Chikhaoui, Marcillat & Sani (1988) in a combined numerical and experimental study found a sequence of transitions in a tall three-dimensional cavity with two differentially heated vertical walls and all other walls perfectly conducting. For increasing Grashof number, based on the smallest horizontal dimension of the cavity, the sequence found was: uni-cellular flow, multi-cellular flow, oscillations, uni-cellular flow (reverse transition), oscillations with a steady amplitude (Hopf bifurcation) and a single frequency, oscillations with two frequencies and finally a chaotic regime with no distinct frequencies. All these transitions occurred in the range $10^4 \leqslant Gr \leqslant 1.76 \times 10^6$, where

$$Gr = g\beta(T_h - T_c) H^3/\nu^2$$

(T_h, T_c being the temperatures of the hot and the cold walls, respectively, and H the width of the cavity). In the study of Paolucci & Chenoweth (1989) a sequence of transitions was also found, starting from the periodic regime and moving successively to a quasi-periodic, a chaotic (weakly turbulent) and a fully turbulent regime. They also proposed that for a cavity with aspect ratio 1, the first bifurcation from steady to periodic convection is an instability due to gravity waves, while the second one, from the periodic to quasi-periodic is due to an instability in the boundary layers, along the vertical walls. Each of these bifurcations is associated with one distinct frequency and its harmonics and their values are incommensurate.

Finally, it should be mentioned that there are also several studies where oscillations for low-Prandtl-number fluids such as liquid metals have been reported, mostly for shallow cavities (aspect ratio $A = H/W < 1$), heated from the sides. Typical examples are, among others, the numerical works by Roux, Bontoux & Henry (1985) and the more recent ones by Gervasio *et al.* (1990) and Afrid & Zebib (1990). They found various transitions, either to multi-cellular or oscillatory states, depending on the aspect ratio of the cavity, the Prandtl and Grashof numbers. However, their results cannot be quantitatively compared to those of the previously mentioned works which all considered air as the fluid, as also does the present work. The Prandtl number of air is outside the range of Pr considered by Roux *et al.* (1985) and Afrid & Zebib (1990). Nevertheless, the basic trends are similar.

While the periodic natural convection in cavities has recently been studied in detail to understand the basic mechanisms, the present work will show that similar periodic behaviour is also encountered in cavities where the heat transfer is due to mixed convection. More specifically, in the cavity to be studied here, the heating is due to an isolated heat source of length L_s, generating a constant heat flux q_s'' per unit area and located on a vertical wall of the cavity, with its centre at a distance d_s from the bottom. The fluid is air, with a coefficient of thermal expansion β, kinematic viscosity ν and thermal conductivity k_f. The natural convective flow due to the source interacts with an external cold air flow which enters the cavity at a mean inlet velocity v_i through an opening of height H_i and exits through a similar opening on the opposite vertical wall. It is found that at a certain critical value of the modified Grashof number $Gr = (g\beta\Delta T H_i^3)/\nu^2$ (or the modified Rayleigh number $Ra = (g\beta\Delta T H_i^3)/(\nu\alpha_f)$), where g is the gravitational acceleration and $\Delta T = q_s'' H_i/k_f$ is based on the heat input of the source, the flow becomes periodic and exhibits a

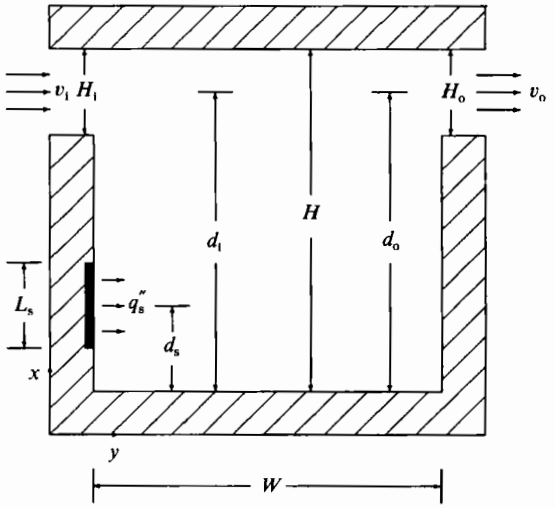

FIGURE 1. The geometry of the flow configuration under consideration, along with the coordinate system.

behaviour very similar to that discussed above, pertaining to pure natural convection. However, the Reynolds number $Re = v_i H_i/\nu$ of the external flow is also found to have an effect on the oscillating flow, as expected.

2. Mathematical formulation

2.1. *Governing equations*

The configuration considered here is shown in figure 1, with all the geometry parameters. The fluid is air, with a Prandtl number $Pr = \nu/\alpha_f = 0.733$, where α_f is the fluid thermal diffusivity, and is considered as incompressible. The fluid flow and heat transfer are governed by the continuity, Navier–Stokes and energy equations. The effect of thermal buoyancy due to the heat input is taken into account for the air flow inside the enclosure. The Boussinesq approximations are applied for the density variations. The compressibility work and the viscous dissipation terms are neglected in the energy equation. With the foregoing assumptions, the equations for the two-dimensional flow under consideration are first written in terms of the primitive variables, i.e. the velocity components u, v, the pressure p and the temperature T. Then, the equations are non-dimensionalized using H_i as the characteristic length, v_i as the characteristic velocity and v_i/H_i as the characteristic time. By the elimination of the pressure, the equations are obtained in terms of the dimensionless stream function Ψ (where $U = \partial\Psi/\partial Y, V = -\partial\Psi/\partial X$), vorticity $\Omega = \partial V/\partial X - \partial U/\partial Y$ and temperature $\theta = (T - T_i)/\Delta T$. Hence, the stream function–vorticity formulation for the problem in conservative form is:

vorticity transport equation (fluid region)

$$\frac{\partial\Omega}{\partial\tau} + \nabla\cdot(\boldsymbol{V}\Omega) = -\frac{Gr}{Re^2}\frac{\partial\theta}{\partial Y} + \frac{1}{Re}\nabla^2\Omega; \tag{1}$$

stream function equation (fluid region)

$$\nabla^2\Psi = -\Omega; \tag{2}$$

Energy equation (both regions)

$$\rho C_P\left[\frac{\partial\theta}{\partial\tau}+\nabla\cdot(V\theta)\right]=\nabla\cdot\left[\frac{k}{a_f}\frac{1}{Re\,Pr}\nabla\theta\right]. \tag{3}$$

In these equations, $V=(U,V)$ is the dimensionless velocity vector, with U the vertical and V the horizontal component, respectively. In the energy equation, the density ρ, the specific heat at constant pressure C_P and the thermal conductivity k may refer to either the fluid or the solid, since this equation is valid over the entire domain, including both the solid and the fluid regions. The properties of the solid are denoted by the subscript s and those of the fluid by the subscript f. When the equation is solved in the solid region, the ratio of the thermal diffusivities $r_\alpha=\alpha_s/\alpha_f$ will arise as a parameter when the equation is divided through by ρC_P.

2.2. *Boundary conditions*

The no-slip conditions at the walls $U=V=0$ lead to the condition $\Psi=$ constant. Thus, at the ceiling of the enclosure, Ψ is arbitrarily specified as zero. If the dimensionless mass flow rate at the inflow is taken equal to 1, mass conservation requires that $\Psi=1$ at the lower horizontal boundary, or floor, as well as at the portion of the vertical walls that lies below the inflow and outflow channels. The vorticity is not known in advance at the walls and will be computed as part of the numerical procedure. At the inflow opening, the conditions, assuming uniform flow, are

$$U_i=0,\quad V_i=1,\quad \Psi_i=1-[X-(d_i^*-\tfrac{1}{2})],\quad \Omega_i=0, \tag{4}$$

where d_i^* is the dimensionless distance of the midplane of the inlet channel from the bottom of the cavity. For the boundary condition at the outflow, all the gradients in the horizontal direction, denoted by a subscript o, are taken as zero, to represent developed flow and thermal fields. The vertical velocity component is also zero. Thus

$$U_o=0,\quad (\partial V/\partial Y)_o=(\partial\Psi/\partial Y)_o=(\partial\Omega/\partial Y)_o=0, \tag{5}$$

and the boundary conditions for the temperature distribution is

$$\partial\theta/\partial n=0\quad\text{at the outer walls,} \tag{6}$$

where n is the direction normal to the wall. This condition is also applied at the outflow, with Y replacing n, while at the inflow $\theta=0$. Then, at the interior walls (solid–fluid interfaces), the continuity in the heat flux requires that

$$(\partial\theta/\partial n)_f=r_k(\partial\theta/\partial n)_s+C,\quad\text{where}\quad C=\begin{cases}-1 & \text{on the heat source}\\ 0 & \text{on other surfaces,}\end{cases} \tag{7}$$

where, again, n is the direction normal to the interface, $r_k=r_\alpha r_c=k_s/k_f$ is the thermal conductivity ratio and r_c is the ratio of the thermal capacities.

3. Numerical procedure

The computational domain, including both the fluid and the solid wall region, is discretized by using a non-uniform grid with 49 grid points in the horizontal direction and 45 points in the vertical direction. The points are more closely spaced in regions adjacent to the walls, where large temperature and velocity gradients are expected to develop. A finer grid (89×97) was also used for comparison, by doubling the number of grid points in each direction. At these grid dimensions the results were

found to be largely grid independent. The governing equations were discretized and converted into systems of algebraic equations by integrating over control volumes defined around each grid point, in the manner described in Patankar (1980) and using the power-law approximation for the convective terms. Special equations were derived for the grid points lying on solid–fluid interfaces, by considering energy balances over two partial control volumes, one on the fluid side and one on the solid side and equating the heat fluxes at their common interface. The relevant procedure is described by Papanicolaou & Jaluria (1990*a*).

The numerical procedure is the same as that described by Papanicolaou & Jaluria (1990*b*). The time-dependent vorticity and energy equations are written in the following common form in terms of a dummy variable ϕ:

$$\partial\phi/\partial\tau + \nabla\cdot\boldsymbol{J}^* = S_\phi, \tag{8}$$

where S_ϕ is a source term in this generic advection–diffusion equation and depends on the variable ϕ. It can easily be realized that

$$S_\phi = \begin{cases} -(Gr/Re^2)(\partial\theta/\partial Y) & \text{in the vorticity equation} \\ 0 & \text{in the energy equation.} \end{cases} \tag{9}$$

The symbol $\boldsymbol{J}^*$ represents the total (convective + diffusive) flux vector (dimensionless for our purposes), which is defined as

$$\boldsymbol{J}^* = \boldsymbol{V}\phi - \Gamma\nabla\phi. \tag{10}$$

In this definition, Γ is a diffusion coefficient which depends on the type of equation to be solved. Comparing (10) with (1) and (3), it is seen that

$$\Gamma = \begin{cases} 1/Re & \text{in the vorticity equation} \\ 1/(RePr) & \text{in the energy equation (fluid region)} \\ r_a(1/RePr) & \text{in the energy equation (solid region).} \end{cases} \tag{11}$$

The alternating direction implicit (ADI) method was employed in the solution of (8). The equation is first integrated over each control volume ΔV and the space derivatives are removed. The time discretization is then carried out in two steps, involving three successive time levels, namely $\tau^{(k)}$, $\tau^* = \tau^{(k)} + \frac{1}{2}\Delta\tau$ and $\tau^{(k+1)} = \tau^{(k)} + \Delta\tau$: at $\tau^* = \tau^{(k)} + \frac{1}{2}\Delta\tau$:

$$\frac{\phi_P^* - \phi_P^{(k)}}{\frac{1}{2}\Delta\tau}\Delta V + a_N(\phi_P^* - \phi_N^*) - a_S(\phi_S^* - \phi_P^*)$$

$$+ a_E(\phi_P^{(k)} - \phi_E^{(k)}) - a_W(\phi_W^{(k)} - \phi_P^{(k)}) = \int_{\Delta V} S_\phi \, dV;$$

at $\tau^{(k+1)} = \tau^* + \frac{1}{2}\Delta\tau$:

$$\frac{\phi_P^{(k+1)} - \phi_P^*}{\frac{1}{2}\Delta\tau}\Delta V + a_N(\phi_P^* - \phi_N^*) - a_S(\phi_S^* - \phi_P^*)$$

$$+ a_E(\phi_P^{(k+1)} - \phi_E^{(k+1)}) - a_W(\phi_W^{(k+1)} - \phi_P^{(k+1)}) = \int_{\Delta V} S_\phi \, dV.$$

By separating the unknown from the known values at each of the time levels τ^* and $\tau^{(k+1)}$, tridiagonal systems of algebraic equations are obtained and solved. The successive over-relaxation (SOR) method was used in the solution of the stream function equation (Jaluria & Torrance 1986). This is a very efficient method for large

systems of linear algebraic equations characterized by sparse matrices, such as the stream function equation in this problem. With ω denoting the over-relaxation factor, the expression obtained for the value of the stream function at any point i,j of the flow field is

$$\Psi_{i,j}^{(n+1)} = \Psi_{i,j}^{(n)} + \left(\frac{\omega}{r_i H_{i,j}^2 + r_j}\right)\left[\left(\frac{r_i H_{i,j}^2}{1+r_i}\right)(\Psi_{i-1,j}^{(n+1)} + r_i\,\Psi_{i+1,j}^{(n)}) + \left(\frac{r_j}{1+r_j}\right)(\Psi_{i,j-1}^{(n+1)} + r_j\,\Psi_{i,j+1}^{(n)}) - (H_{i,j}^2 r_i + r_j)\,\Psi_{i,j}^{(n)} + \tfrac{1}{2}\Omega_{i,j}(\delta Y)_j^2\right] \quad (12)$$

for $i = 1, 2, \ldots, i_{\max} - 1$ and $j = 1, 2, \ldots, j_{\max} - 1$. In the above expression,

$$H_{i,j} = \delta Y_j / \delta X_i$$

is the local grid aspect ratio and $r_i = \delta X_{i-1}/\delta X_i, r_j = \delta Y_{j-1}/\delta Y_j$ are the ratios between two adjacent grid spacings in the X- and Y-directions, respectively. The wall vorticity is updated at each time step, using finite-difference approximations (Roache 1972). Both first-order and second-order formulae have been used. The second-order formula is

$$\Omega_{\mathrm{w}} = \frac{7\Psi_{\mathrm{w}} - 8\Psi_{\mathrm{w}+1} + \Psi_{\mathrm{w}+2}}{2(\Delta n)^2} + O(\Delta n)^2, \quad (13)$$

where Δn is the distance of the first node far from the wall, the subscript w denotes the value of the vorticity at the wall and $\mathrm{w}+1, \mathrm{w}+2$ are the values at the two adjacent nodes. The above equation, however, is valid only for uniform grid regions and, thus, in non-uniform grid regions a first-order formula was used, which is (Jaluria & Torrance 1986)

$$\Omega_{\mathrm{w}} = -\frac{2(\Psi_{\mathrm{w}+1} - \Psi_{\mathrm{w}})}{(\Delta n)^2} + O(\Delta n). \quad (14)$$

The code was validated by solving the benchmark problem of natural convection in a closed cavity, indicating a close agreement as described by Papanicolaou & Jaluria (1990*b*).

Since our purpose was to study the periodic regime, which is usually obtained after an initial transient, we tried to use the largest possible value of the time step, without encountering numerical stability problems, in order to reach the periodic regime fast. This value was found to be 0.1. Later the time step was reduced to study its effect on the results. For the first computation, the initial condition was the solution obtained at the highest value of Gr that resulted in a steady, laminar flow field at the same value of Re. Then, once the periodic regime was reached, for certain values of the governing parameters, the solution obtained could be used as an initial condition for the next highest value of Gr for steady flow.

It should also be noted that the geometric parameters shown in figure 1 were kept fixed at the following non-dimensional values, which are typical of laminar flow in a small enclosure such as those encountered in electronic circuitry: $H = W = 4.0$; $L_{\mathrm{s}} = d_{\mathrm{s}} = H_{\mathrm{o}} = H_{\mathrm{i}} = 1.0$; $d_{\mathrm{i}} = d_{\mathrm{o}} = 3.5$, where H is the height and W the width of the cavity. Since the problem treated here is conjugate, values must also be chosen for the thermal diffusivity and thermal capacity ratios (solid/fluid), r_α and r_c respectively. In this work, the effect of these parameters will not be studied and thus their values are fixed at: $r_\alpha = 0.8$ (typical for materials such as steel or aluminium) and $r_c = 1.0$. For $r_\alpha = 0$, the adiabatic wall case is obtained, which was also found to yield oscillatory results (Papanicolaou & Jaluria 1990*b*).

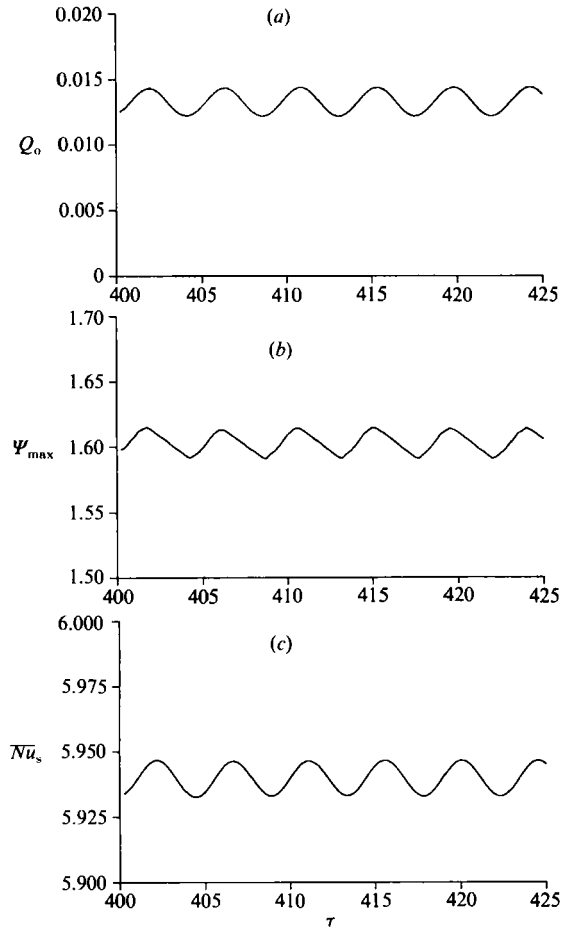

FIGURE 2. Typical time variation for $Re = 100$ and $Gr/Re^2 = 35$ of (*a*) outflow heat flux; (*b*) maximum stream function; (*c*) average Nusselt number at the source.

4. Results and discussion

4.1. *Effect of the Grashof number*

First, the Reynolds number is fixed at the value $Re = 100$ and the Grashof number Gr is varied. This variation is expressed in terms of the parameter Gr/Re^2, which is the overall Richardson number (Turner 1973), or, for simplicity in what follows, the Richardson number. It must, however, be kept in mind that an increase in the value of this parameter is due to an increase in the value of Gr. As was reported by Papanicolaou & Jaluria (1990*a*), laminar steady results can be obtained for up to a value of $Gr/Re^2 = 30$ for $Re = 100$. Some low-amplitude oscillations were present near steady state but these were later damped out when the time step was decreased. This damping occurs up to $Gr/Re^2 = 32$, but at $Gr/Re^2 = 33$, the oscillations persist and this is where the periodic regime starts. When various quantities are monitored with time, such as the total heat flux Q_0 at the outflow channel, the maximum stream function Ψ_{max} and the average Nusselt number at the source $\overline{Nu}_s = \bar{h}H_i/k_f$, $\bar{h}$ being the average convective heat transfer coefficient, after an initial transient, a periodic variation is observed, characterized by constant amplitude and a single frequency, as shown in figure 2. The amplitude of the oscillations increases with the Grashof

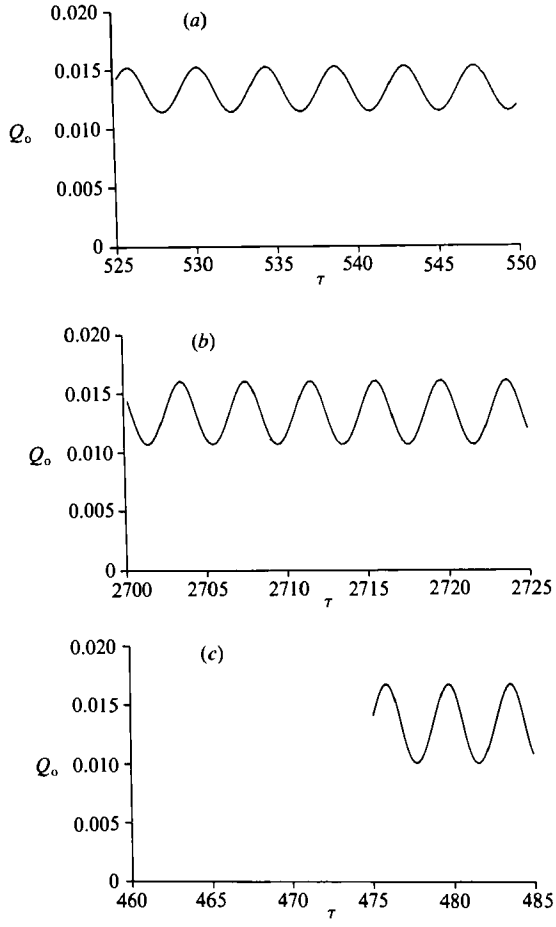

FIGURE 3. Time variation of the outflow heat flux Q_0, demonstrating the effect of increasing Gr/Re^2 on the amplitude of the oscillations, for $Re = 100$ and (*a*) $Gr/Re^2 = 40$; (*b*) 50; (*c*) 60.

number, as verified by the time variation of Q_0 at different Grashof numbers shown in figure 3.

The presence of the single frequency is verified by the power-spectrum analysis shown in figure 4. The pattern of this periodic variation may look quite different, depending on the chosen time step $\Delta\tau$. Although the periodicity is evident, even at large time steps, the actual frequency and the actual amplitude can only be determined when the time step is decreased to smaller values. As expected, it was found that there is a minimum value of the time step, below which it has no further effect. The output is then found to be sinusoidal and dominated by a single frequency. This is clearly depicted in figure 5. The dimensionless time step used initially was $\Delta\tau = 0.1$. It was then decreased by a factor of 4, to the value $\Delta\tau = 0.025$ and then, again, by a factor of 4 to $\Delta\tau = 0.00625$. For $\Delta\tau = 0.1$, there seems to be an almost sinusoidal variation; however, the actual frequency is not captured and a lower frequency is obtained instead. This is an 'aliasing' phenomenon, where the frequency of a periodic function may appear like one of its lower harmonics if the sampling rate of the function is not high enough. The amplitude, however, is very close to the actual one, which is obtained using a time step equal to 0.00625. When the time step is reduced to $\Delta\tau = 0.025$, a higher frequency is captured, while the

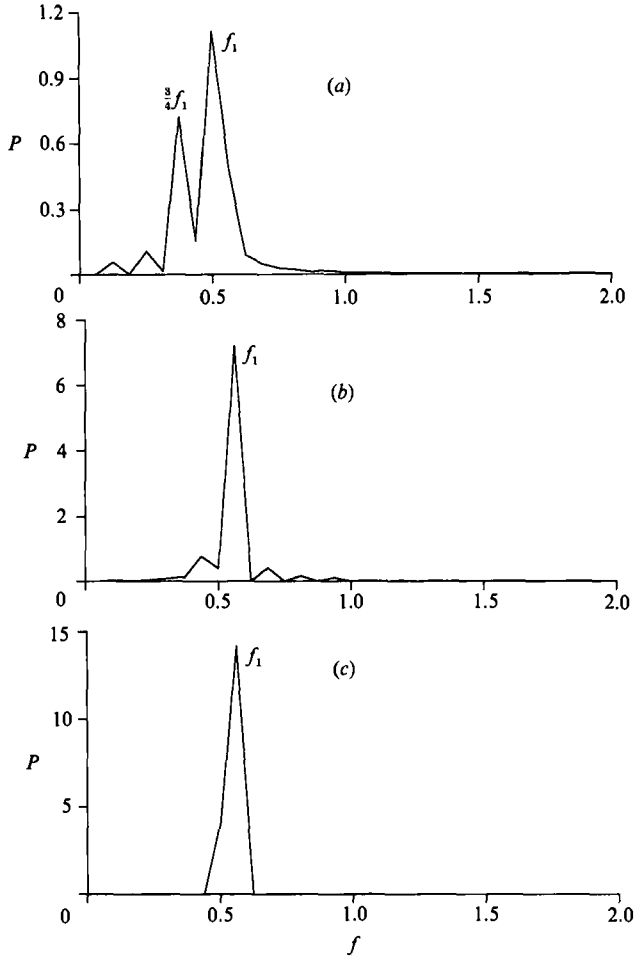

FIGURE 4. Power-spectrum analysis of the time variation of the outflow heat flux. The horizontal axis is the dimensionless frequency and (*a*) $Gr/Re^2 = 35$; (*b*) 40; (*c*) 50.

lower frequency is also present and the amplitude of the oscillations is found to vary periodically. This pattern is similar to the phenomenon of 'beating' in the theory of mechanical vibrations. The appearance of a periodically varying amplitude however, is still misleading, since with a further reduction in the time step $\Delta\tau$ to 0.00625, the amplitude is seen to remain constant. Only the higher frequency now remains and, as was shown in figure 2, the variation with time is sinusoidal. Similar time plots showing beating patterns were also obtained in the results of LeQuéré & Roquefort (1985). They observed the existence of two distinct frequencies and they attributed the presence of the lower frequency to internal wave motion. Although this is very likely, there is also a possibility that this lower frequency might simply be of numerical origin and could have been eliminated if the sampling rate of the values were increased by using a smaller time step, as is seen to be the case in our results. For Richardson number Gr/Re^2 less than 60, the time step $\Delta\tau = 0.00625$ was found to be adequate to resolve the dominant frequency. However, at $Gr/Re^2 = 60$, the time step had to be reduced to $\Delta\tau = 0.00125$ for accurate determination of both the amplitude and the frequency.

From these plots, the time period of the sinusoidal variation can be found and the

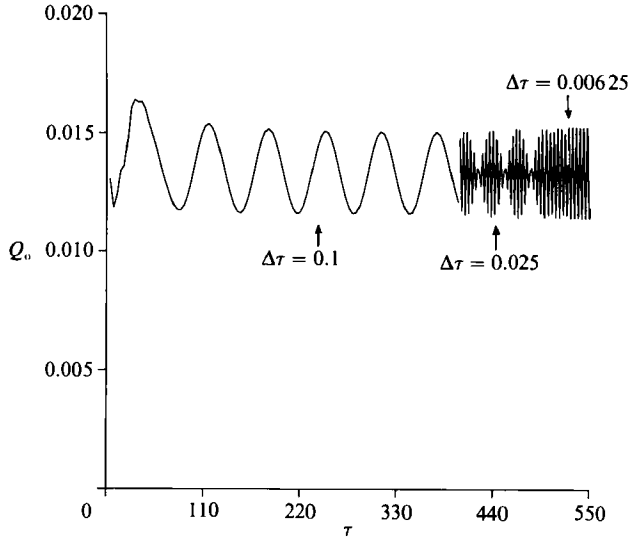

FIGURE 5. Effect of the time step $\Delta\tau$ on the time variation of the outflow heat flux, for $Re = 100$ and $Gr/Re^2 = 40$. Only at the value $\Delta\tau = 0.00625$ is an accurate pattern of the output obtained, both in terms of the frequency and the amplitude.

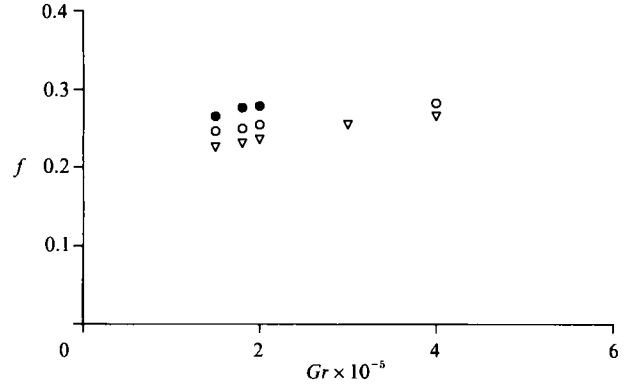

FIGURE 6. Variation of the dimensionless frequency of the oscillations in the outflow heat flux with the Grashof number Gr, at various Reynolds numbers: ●, $Re = 80$; ○, 90; ▽, 100.

inverse of this value taken as the frequency of the signal. Alternatively, a fast-Fourier transform (FFT) may be applied to the data and the power-spectrum density P obtained, to determine the fundamental frequency. This is shown in figure 4 for the periodic behaviour of the outflow heat flux. The dominance of one single frequency for each value of Gr/Re^2, along with its harmonics, is obvious. A sample of $2^7 = 128$ data points was found to be adequate to compute the fundamental frequency, denoted by f_1 in figure 4. Increasing the number of points to $2^9 = 512$ simply gave a sharper peak for f_1 but did not show any other frequencies.

As the Grashof number is increased further, the amplitude of the oscillations, as well as the frequency, increases. This is clearly shown in figure 3, where the presence of a single, dominant frequency is indicated. The increase in the frequency of the oscillations with Gr/Re^2 is shown in figure 6 and the increase in the amplitude in figure 7. As will be shown below, the frequencies in figure 6 do not vary with the

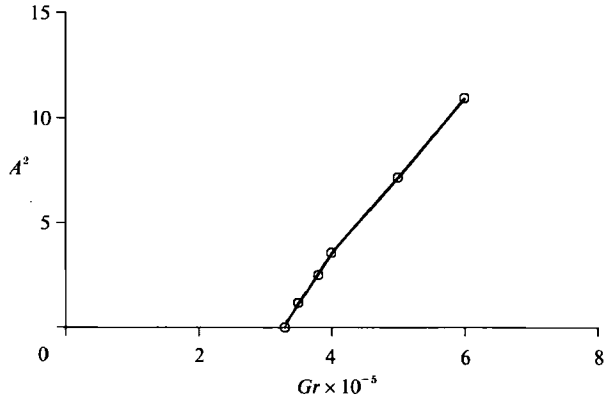

FIGURE 7. Variation of the amplitude of the oscillations in the outflow heat flux with Gr, at $Re = 100$. The linear variation is clearly shown at slightly supercritical values of Gr.

square root of the Grashof number, as is the case for periodic natural convection problems, but rather with a smaller power of Gr. Clearly, from the same figure one may conclude that an increase in the Reynolds number leads to lower frequencies for the same Gr. In figure 7, the slightly supercritical values of Gr at $Re = 100$ are shown to give amplitudes A that can be approximated by a straight line. This is consistent with the theory of Hopf bifurcation and also with the results of LeQuéré & Roquefort (1986), where an extrapolation of the straight line towards lower values of Gr was used to determine the critical value of Gr. Here, with a similar approach, we find $Gr_{cr} = 3.3 \times 10^5$ for $Re = 100$. As the values of Gr are increased further beyond the critical point, the slope of the line is found to change.

4.2. *Effect of the Reynolds number*

The next set of results was obtained by keeping the Richardson number fixed at $Gr/Re^2 = 50$ and varying the Reynolds number in the range 100–2500. It was found that an increase in the Reynolds number has a stabilizing effect. Oscillations were observed for up to about $Re = 200$. For higher values, a steady solution was obtained. This shows that there is a critical value of Re above which the external flow cannot reinforce the oscillations that occur at the centre of the cavity. Instead, it is so strong that it damps out any disturbances in the flow.

Another set of results can be obtained by keeping the Grashof number fixed at $Gr = 5 \times 10^5$ and varying the Reynolds number in the range 50–200. Again, for higher values of Re the solution was found to be steady. The critical value was found to be $Re_{cr} = 125$ and this corresponds to a Richardson number $Gr/Re^2 = 32$. This is very close to what was found when the Reynolds number was fixed at $Re = 100$ and the Richardson number was varied. The fact that the Reynolds number has a stabilizing effect verifies that the observed instability is not a flow instability, but rather a thermal one whose nature is discussed in detail below.

Other computational runs were made for $Re = 80$ and 90 and it was found that the critical Richardson number for these values lies near $Gr/Re^2 = 34$. However, the frequencies of the oscillations could not be determined accurately in the beginning, since a clearly defined period does not appear unless Gr/Re^2 increases to values higher than 35, at least with the 45×49 grid. The oscillations that develop near the critical value are very irregular both in terms of amplitude and frequency.

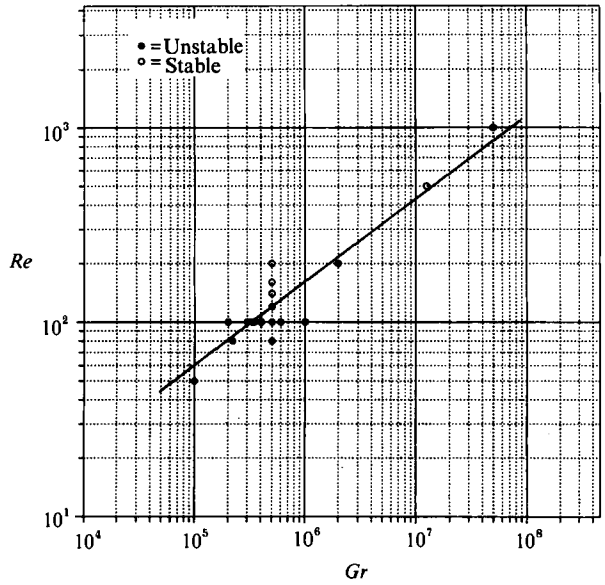

FIGURE 8. Stability diagram of the mixed convection flow in the cavity considered here, for the transition from steady to periodic flow.

4.3. *Frequency of the oscillations*

The critical frequency is found to be approximately equal to 0.17, both for $Re = 80$ and 90 and about 0.18 for $Re = 100$, although this is a very crude approximation for the reasons mentioned above. As the critical value of Gr for these values of Re is approached, the oscillations are of very low amplitude and the time required for the steady-periodic state to be reached increases. This is preceded by oscillations of varying amplitude and frequency. For $Re = 100$, it is only at about $Gr/Re^2 = 35$ where a clearly defined period and amplitude arise early. The frequency was found to increase with the Grashof number and decrease with the Reynolds number, as seen in figure 6. Taking into account the relevant effect of both Gr and Re in determining the frequency of the oscillations, and using data for $Gr = 3.5\text{–}6 \times 10^5$ and $Re = 80\text{–}120$, the following approximate correlation was derived for the dimensionless frequency f:

$$f = 0.23 Gr^{0.3} Re^{-0.8}. \tag{15}$$

The effect of the Reynolds and Grashof numbers on the stability can be represented by a stability diagram of the form shown in figure 8. From the results presented here, there is strong evidence that the boundary separating the stable from the unstable region can be very closely approximated by a straight line. This is qualitatively similar to the stability diagram of Chen, Moutsoglou & Armaly (1982) for the thermal mode of instability, in flows over isothermal inclined plates. As will be further discussed later, the instability in the present work is also of a thermal nature.

In order to compare our frequencies with those of natural convection, the differences in the length- and timescales have to be taken into account. In Briggs & Jones (1985) and LeQuéré and Alziary de Roquefort (1985, 1986), the lengthscale is the width of the cavity W, while the timescale is the thermal diffusion scale. In our case the lengthscale is the height H_1 of the inflow opening and the timescale is based on the inlet velocity v_1. Therefore, if f_n is the dimensionless frequency in the natural

convection case and f_m is the corresponding frequency in the mixed convection case, the ratio of the dimensional frequencies, denoted by primes, will be

$$\frac{f'_m}{f'_n} = \left(\frac{f_m}{f_n}\right)\left(\frac{H_i}{W}\right)^2\left(\frac{1}{RePr}\right). \tag{16}$$

Since $H_i/W = \frac{1}{4}$, the above equation becomes

$$\frac{f'_m}{f'_n} = \left(\frac{f_m}{f_n}\right)\left(\frac{1}{16}\right)\left(\frac{1}{RePr}\right). \tag{17}$$

In the natural convection case, the critical frequency is approximately 0.255 and in the mixed convection case, for $Re = 100$, it is found to be approximately 0.18, both in non-dimensional values. A simple calculation from (17), for $Re = 100$ and $Pr = 0.733$, gives $f'_n = 1661 f'_m$. Therefore, the frequencies for natural convection flow in the cavity are much higher than those for mixed convection, at the critical value of the Grashof number. The highest value of the Richardson number that gives consistent trends for the variation of the frequency is $Gr/Re^2 = 60$, for grid dimensions 45×49 and a time step of $\Delta\tau = 0.001\,25$. Above this value, the oscillations become irregular and it is necessary to use a finer grid to investigate whether higher-order transitions are taking place.

4.4. *Effect of the grid dimensions*

Many of the results presented here were obtained with a 45×49 grid. The final periodic state could be obtained using different starting time steps and initial conditions, the latter being obtained from lower-Grashof-number solutions. The same frequency was always obtained at the end, for all initial conditions used and even starting with the fluid at rest. It was important though to ensure that the time step was sufficiently small once the periodic regime was reached, as figure 5 illustrates. However, in order to confirm the validity of our numerical prediction of unsteadiness and periodicity in this problem, different grid dimensions were considered. Initially, the number of grid spacings in each direction was doubled, so that the mesh became 89×97. Since the grid size is now reduced, the time step also had to be reduced for numerical stability reasons. With a time step $\Delta\tau = 0.01$, the numerical scheme eventually results in a periodic solution again, even for the smaller grid dimensions. However, the values of the frequency and the amplitude of the oscillations are found to be somewhat different from those obtained earlier. The fact that the finer grid did not damp out the oscillations, but showed higher amplitudes instead, was a confirmation of the belief that the oscillations were of physical and not of numerical origin. As a matter of fact, the oscillations were better captured by the finer grid.

For a better understanding of the effect of the grid dimensions, other values were also considered and the complete results are shown in table 1. It can be observed that some of the results, such as the frequency and especially the amplitude of the oscillations, are extremely sensitive to the grid size and their values vary significantly with the grid. Other results such as Ψ_{max}, Q_o, $\overline{Nu}_s$ and $\theta_{s,max}$ are fairly well predicted with the 45×49 grid (within 3.5% error or less) compared to the 111×121 grid. However, the same accuracy for the frequency and the amplitude of the oscillations can only be achieved with the 89×97 grid.

This sensitivity of the oscillatory results to the grid size was also found in the numerical results of Jones & Briggs (1986). Their frequency was approximately 4%

Grid	23×25	45×49	67×73	89×97	111×121
f	No oscill.	0.231	0.242	0.249	0.253
Ampl. in Q_0 ($\times10^3$)	0	1.975	3.350	3.975	4.075
Q_0	0.01338	0.01337	0.01375	0.01385	0.01395
Ampl./Q_0 %	0	14.77	24.36	28.88	29.21
Ψ_{max}	1.907	1.652	1.693	1.699	1.695
$\theta_{s,max}$($\times10^2$)	14.625	18.362	18.863	18.974	19.029
$\overline{Nu}_s$	7.188	5.886	5.722	5.711	5.712

TABLE 1. Sensitivity of selected results on the grid dimensions for a source on the left-hand wall, at $Re = 100$ and $Gr/Re^2 = 40$

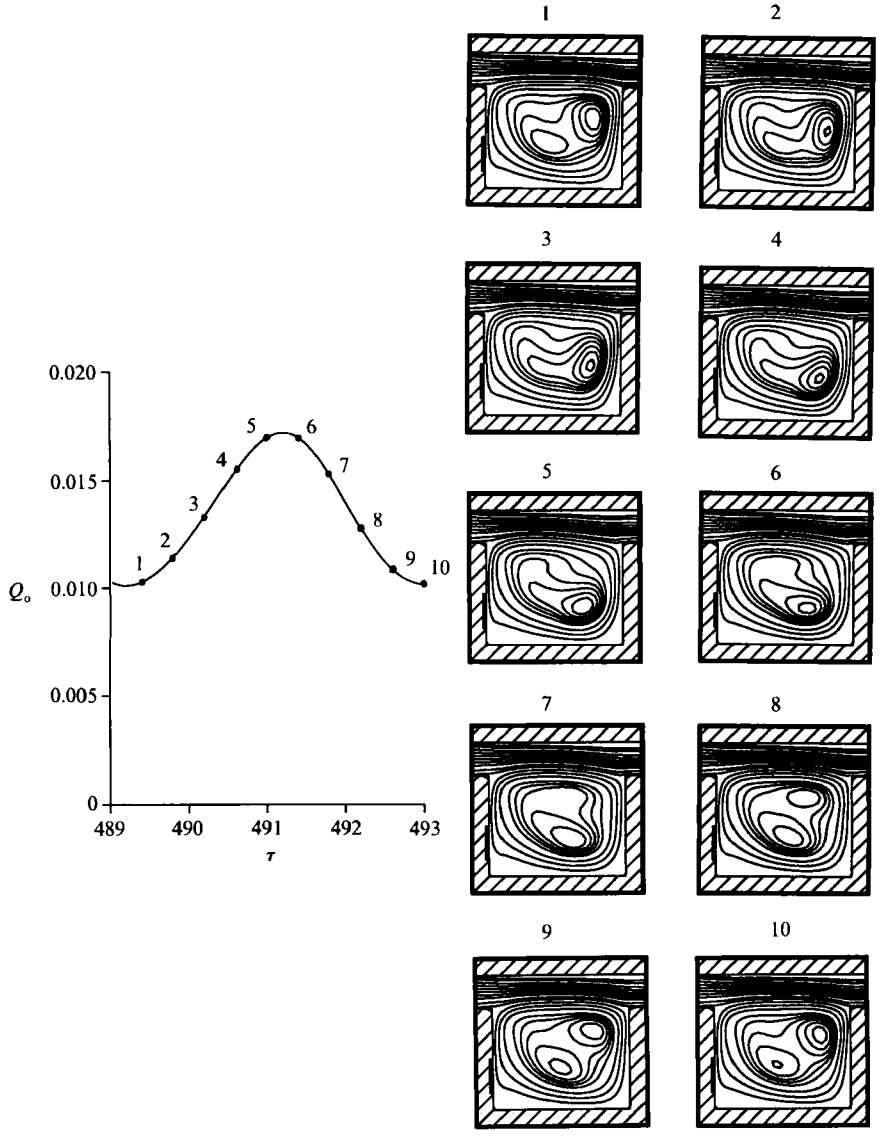

FIGURE 9. Streamlines at ten different time instants within a cycle of the oscillations, for $Re = 100$ and $Gr/Re^2 = 60$.

higher for a 127×127 grid, than that for a 63×63 grid. The value obtained with the finer grid was closer to the experimentally measured frequency. Also, Gervasio *et al.* (1990) found that the coarse grid underpredicted the amplitude of the oscillations by 30%. In the present work too, the frequencies and amplitudes obtained with the finest grid are expected to be closer to the actual values. However, the basic trends can still be observed and analysed with the coarser 45×49 grid, which requires significantly less computational effort.

4.5. *Nature of the instability*

The streamline patterns at different time instants within a cycle of the oscillations reveal more details about the behaviour of the fluid in the cavity. As figure 9 shows, the flow field is affected only at the centre of the cavity. The cells corresponding to the highest streamline values undergo a circulatory motion at the right-hand half of the cavity. At some point, they also split into two and then recombine again. Similarly, the isotherms shown in figure 10 demonstrate a periodic motion of certain, low-temperature contour lines at the right-hand half of the cavity, denoted by the letters A and B. These motions have a very small effect on the rest of the flow field. At the region next to the right-hand vertical wall, the cooling effect of the external flow penetrates deeper downward at the Grashof number $Gr = 6 \times 10^5$, as shown in figure 10, and then towards the interior of the cavity. As the cold fluid cells are forced to recirculate, they gradually get heated, both from the hot fluid of the thermal plume of the source and from the bottom surface of the enclosure, which is at a higher temperature.

In the steady, laminar results of Papanicolaou & Jaluria (1990*a*), the heat transfer at the bottom of the cavity was shown to be from the wall to the fluid. This causes the two low-temperature isotherms A and B to move backwards towards the right-hand wall just before the beginning of a new cycle. The penetration of the cooling effect downward and along the right-hand wall was not observed for low values of the Grashof number which gave a laminar, steady solution (Papanicolaou & Jaluria 1990*a*) and it is enhanced at higher values of Gr, because the region affected by the heat source gradually becomes thinner. This is why the instability is observed at high values of Gr/Re^2. The fact that there is heating from below in this problem, as was explained above, leads one to believe that the instability is of the Rayleigh–Bénard type. Although the effect of heating from below may play some role in the observed instability, it is not the only cause, since even in the case of the cavity with adiabatic walls (Papanicolaou & Jaluria 1990*b*), it was shown that the solution becomes periodic as the Richardson number Gr/Re^2 exceeds a certain, critical value. Therefore, it can be claimed from the above that the numerically predicted unsteadiness originates from thermal disturbances occurring at the right-hand half of the cavity, opposite to the wall where the heat source is mounted and has the form of a travelling wave instability.

4.6. *Additional effects*

Several other variations of the problem, due to changes in the physical or geometric parameters are possible. One of the physical parameters is the thermal diffusivity ratio r_α. For the special case $r_\alpha = 0$ (adiabatic walls) the critical value for the transition was found to be lower (Papanicolaou & Jaluria 1990*b*); more specifically $(Gr/Re)^2_{cr} = 20$ for $Re = 100$. This indicates that at least for this particular cavity configuration, by allowing conduction through the walls, i.e. by making the problem conjugate, the periodic regime is delayed. Alternative configurations have been

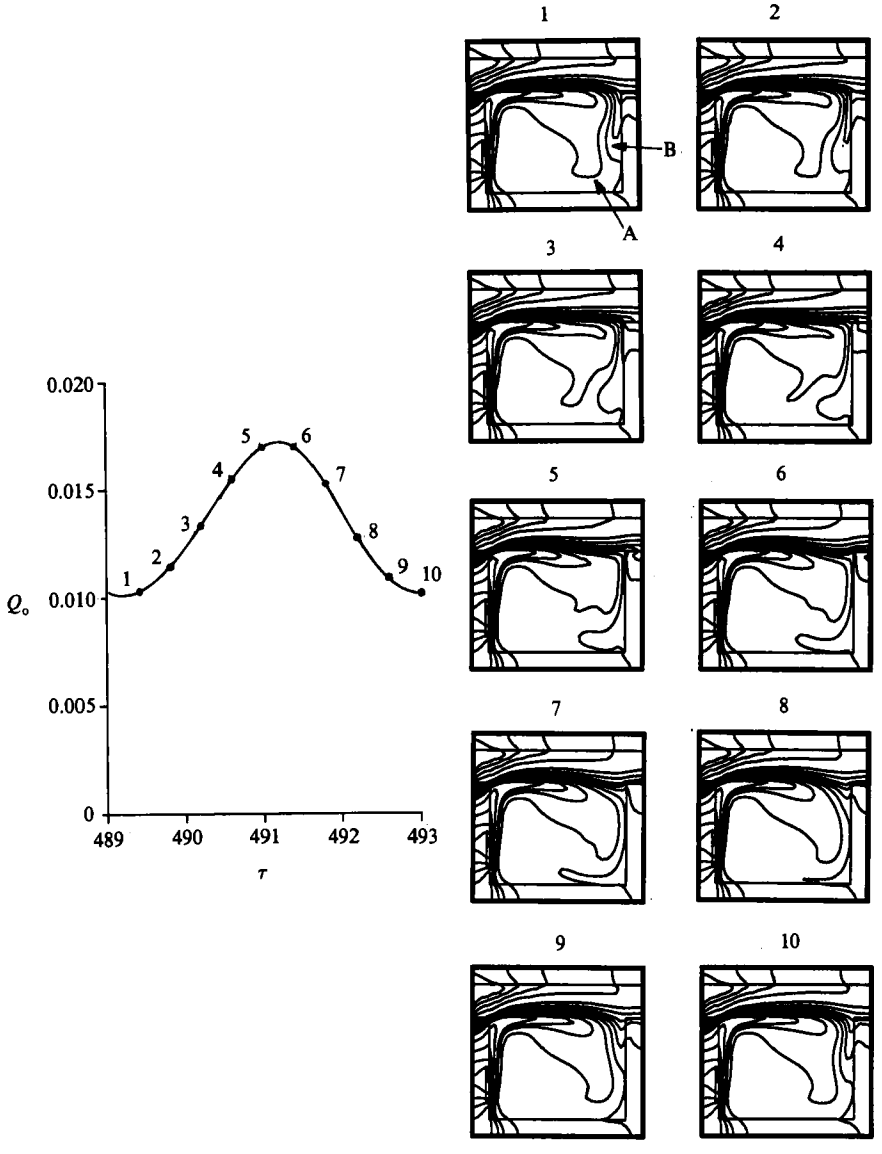

FIGURE 10. Isotherms at different time instants within a cycle of the oscillations, for $Re = 100$ and $Gr/Re^2 = 60$. Of particular interest is the motion of lines marked A and B.

investigated by placing the heat source at the bottom surface, at a distance $d_s = 0.5$ from the left-hand wall and also by considering interactions between two sources, located on different surfaces. The case of a single source at the bottom (Papanicolaou & Jaluria 1990*b*) indicated oscillations even at $Gr/Re^2 = 1$ for $Re = 100$. This is due to the instability arising from the heating-from-below circumstance, which has been studied in detail in the literature (Gebhart *et al.* 1988).

The interaction between two sources was studied in three different configurations, with corresponding source locations: (*a*) left- and right-hand wall; (*b*) left-hand wall and bottom; (*c*) right-hand wall and bottom (Papanicolaou & Jaluria 1991). It was observed that the presence of a source at the bottom made the configurations (*b*) and (*c*) even more unstable than the single-source configuration, again due to the heating-

from-below effect. This was confirmed by the presence of higher amplitudes of the periodic oscillations, compared to the single-source configuration. However, when the source on the left-hand wall coexisted with a source on the opposite vertical wall, a more stable situation arose, with steady flow obtained even at $Gr/Re^2 = 50$ for $Re = 100$. It appears that the presence of a heat source on the right-hand wall does not allow the low-temperature fluid to move downward along that wall. This is the phenomenon that was observed in figure 10 and which is believed to be the source of the instability and of the periodic behaviour.

The effect of changing the vertical position of the outflow boundary along the right-hand wall, expressed by the parameter d_0, has not been investigated with respect to the periodic behaviour, but only with respect to steady flows. However, knowing that the cold front motion along the right-hand wall is the destabilizing factor, one can expect that by moving the outflow towards the bottom, the behaviour of the fluid could significantly be affected. In particular, such a variation has been found to cause the recirculation region to reduce in size and the external flow to dominate inside the cavity (Papanicolaou & Jaluria 1990*b*). This will most likely have a stabilizing effect.

The problem studied here is two-dimensional and an important question that arises is how different the behaviour of the system would be in three dimensions. There is already enough evidence (Jones & Briggs 1986; LeQuéré & Alziary de Roquefort 1988; Chikhaoui *et al.* 1988) that the conclusions drawn from the study of a two-dimensional problem are very close to reality. Most experimental studies on similar problems have found that the two-dimensional numerical simulations predicted the transitions and their features (e.g. the frequency of the oscillations) quite successfully. Therefore, based on thee previous observations, it is felt that the results obtained in the present investigation describe the physical phenomena adequately, even though they are restricted to two dimensions. The use of the Boussinesq approximations simplifies the analysis. But the basic features of the flow are not expected to change very much if a non-Boussinesq flow is considered, since the validity of the Boussinesq approximations for air extends over a very wide range of Rayleigh numbers, well beyond the onset of turbulence (Gray & Giorgini 1976). However, non-Boussinesq effects can be important in many practical situations such as fires and the flow is usually turbulent in these situations.

Finally, it should be noted that, as found in a previous study (Papanicolaou & Jaluria 1990*a*), this problem is largely dominated by the thermal boundary conditions, and the inlet and outlet velocity conditions, for a given flow rate, do not have a significant effect on the phenomena taking place inside the cavity. Therefore, it is not expected that imposing different inflow velocity profiles or different outflow boundary conditions will cause major differences in the results. Changes in the aspect ratio, however, may affect the results significantly.

5. Conclusions

The present numerical work predicted that mixed convection of air in a cavity with conducting walls, induced by localized heating, may become unstable beyond a critical value of the Richardson number Gr/Re^2. The effects of this instability in the flow field are contained within a small region at the centre and the region far from the source of the cavity where a circulatory motion of fluid cells takes place. However, the thermal effects are felt over the entire cavity, with the temperature and the heat transfer rate computed from the numerical scheme showing a periodic

variation characterized by a single frequency. This frequency is an increasing function of the Grashof number and a decreasing function of the Reynolds number. In particular, the Reynolds number was found to have a stabilizing effect, suggesting that the instability is of thermal origin. Although the final periodic state could be reached starting from different initial conditions and by using any time step, the time step had to be reduced sufficiently, so as to be able to capture the actual frequencies and amplitudes. The grid dimensions had an effect which was more pronounced on the predicted frequency and amplitude of the oscillations. Increasing grid dimensions showed both an increasing frequency and an increasing amplitude. Although experimental work is needed in order to obtain the actual frequencies, the numerical results of this study are reliable both qualitatively, in describing the physical trends, and quantitatively, in predicting the critical values for the transition.

The authors acknowledge the partial support from NSF, under grant no. CBT-88-03049 and from the Department of Mechanical and Aerospace Engineering, Rutgers University, for this work.

REFERENCES

AFRID, M. & ZEBIB, A. 1990 Oscillatory three-dimensional convection in rectangular cavities and enclosures. *Phys. Fluids* A **2**, 1318–1327.

BRIGGS, D. G. & JONES, D. N. 1985 Two-dimensional periodic natural convection in a rectangular enclosure of aspect ratio one. *Trans. ASME* C: *J. Heat Transfer* **107**, 850–854.

CHEN, T. S., MOUTSOGLOU, A. & ARMALY, B. F. 1982 Thermal instability of mixed convection flow over inclined surfaces. *Numer. Heat Transfer* **5**, 343–352.

CHIKHAOUI, A., MARCILLAT, J. F. & SANI, R. L. 1988 Successive transitions in thermal convection within a vertical enclosure. In *Natural Convection in Enclosure*. ASME HTD, vol. 99, pp. 29–35.

GEBHART, B., JALURIA, Y., MAHAJAN, R. L. & SAMMAKIA, B. 1988 *Buoyancy-Induced Flows and Transport*. Hemisphere.

GERVASIO, C., BOTTARO, A., AFRID, M. & ZEBIB, A. 1990 Oscillatory natural convection in a long horizontal cavity. In *Numerical Simulation of Oscillatory Convection in Low-Pr Fluids*. Notes on Numerical Fluid Mechanics, vol. 27, pp. 136–143. Vieweg.

GRAY, D. D. & GIORGINI, A. 1976 The validity of the Boussinesq approximation for liquids and gases. *Intl J. Heat Mass Transfer* **19**, 545–551.

HALDENWANG, P. 1986 Unsteady numerical simulation by Chebyshev spectral methods of natural convection at high Rayleigh number. In *Significant Questions in Buoyancy Affected Enclosure or Cavity Flows*. ASME HTD, vol. 60, pp. 45–51.

IGARASHI, T. 1978 Natural convective oscillatory flow in an enclosed space, Part 2. *Bull. JSME* **21**, 1022–1030.

IVEY, G. N. 1984 Experiments on transient natural convection in a cavity. *J. Fluid Mech.* **144**, 389–401.

JALURIA, Y. & TORRANCE, K. E. 1986 *Computational Heat Transfer*. Hemisphere.

JONES, D. N. & BRIGGS, D. G. 1986 Periodic two-dimensional cavity flow: effect of linear horizontal thermal boundary condition. In *Significant Questions in Buoyancy Affected Enclosure or Cavity Flows*. ASME HTD, vol. 60, pp. 29–36.

KÜBLBECK, K., MERKER, G. P. & STRAUB, J. 1980 Advanced numerical computations of two-dimensional time-dependent free convection in cavities. *Intl J. Heat Mass Transfer* **23**, 203–217.

LEQUÉRÉ, P. & ALZIARY DE ROQUEFORT, T. 1985 Transition to unsteady natural convection of air in differentially heated vertical cavities. In *Numerical Methods in Laminar and Turbulent Flow*, pp. 841–852. Pineridge.

LEQUÉRÉ, P. & ALZIARY DE ROQUEFORT, T. 1986 Transition to unsteady natural convection of air in differentially heated vertical cavities. In *Significant Questions in Buoyancy Affected Enclosure or Cavity Flows*. ASME HTD, vol. 60, pp. 29–36.

LeQuéré, P. & Alziary de Roquefort, T. 1988 On the existence of multiple periodic solutions of the Boussinesq equations. *C.R. Acad. Sci. Paris* **306**, 681–687.

Paolucci, S. & Chenoweth, D. R. 1989 Transition to chaos in a differentially heated vertical cavity. *J. Fluid Mech.* **201**, 379–410.

Papanicolaou, E. & Jaluria, Y. 1990*a* Conjugate mixed convection from thermal sources in a rectangular cavity. In *Simulation and Numerical Methods in Heat Transfer*. ASME HTD, vol. 157, pp. 29–40.

Papanicolaou, E. & Jaluria, Y. 1990*b* Mixed convection from an isolated heat source in a rectangular enclosure. *Numer. Heat Transfer* A **18**, 427–461.

Papanicolaou, E. & Jaluria, Y. 1991 Convective cooling of multiple electronic components in an enclosure. In *Heat Transfer in Electronic Equipment*. ASME HTD, vol. 171, pp. 29–37.

Patankar, S. V. 1980 *Numerical Heat Transfer and Fluid Flow*. Hemisphere.

Patterson, J. & Imberger, J. 1980 Unsteady natural convection in a rectangular cavity. *J. Fluid Mech.* **100**, 65–86.

Roache, P. J. 1972 *Computational Fluid Dynamics*. Hermosa.

Roux, B., Bontoux, P. & Henry, D. 1985 Numerical and theoretical study of different flow regimes occurring in horizontal fluid layers, differentially heated. In *Macroscopic Modelling of Turbulent Flows*. Lecture Notes in Physics, vol. 230 (ed. U. Frisch, J. Keller, G. Papanicolaou & O. Pironneau), pp. 202–217. Springer.

Staehle, B. & Hahne, E. 1982 Overshooting and damped oscillations of transient natural convection flows in cavities. In *Proc. 7th Intl Heat Transfer Conf.*, Munich, W. Germany, vol. 2, pp. 287–292. Hemisphere.

Turner, J. S. 1973 *Buoyancy Effects in Fluids*. Cambridge University Press.

Winters, K. H. 1987 Hopf bifurcation in the double-glazing problem with conducting boundaries. *Trans. ASME* C: *J. Heat Transfer* **109**, 894–898.